

Temperature dependent electronic correlation effects in GdN

This article has been downloaded from IOPscience. Please scroll down to see the full text article.

2006 J. Phys.: Condens. Matter 18 7337

(<http://iopscience.iop.org/0953-8984/18/31/026>)

View [the table of contents for this issue](#), or go to the [journal homepage](#) for more

Download details:

IP Address: 129.252.86.83

The article was downloaded on 28/05/2010 at 12:34

Please note that [terms and conditions apply](#).

Temperature dependent electronic correlation effects in GdN

A Sharma and W Nolting

Institut für Physik, Humboldt-Universität zu Berlin, Newtonstrasse 15, 12489, Berlin, Germany

E-mail: anand@physik.hu-berlin.de

Received 9 May 2006

Published 21 July 2006

Online at stacks.iop.org/JPhysCM/18/7337

Abstract

We investigate temperature dependent electronic correlation effects in the conduction bands of gadolinium nitride (GdN) based on the combination of many-body analysis of the multi-band Kondo lattice model and the first principles TB-LMTO band-structure calculations. The physical properties like the quasi-particle density of states (Q-DOS), spectral density (SD) and quasi-particle band structure (Q-BS) are calculated and discussed. The results can be compared with spin and angle resolved inverse photoemission spectroscopy (ARIPS) of the conduction bands of GdN. A redshift of 0.34 eV of the lower band edge ($T = T_c \rightarrow T = 0$) is obtained and found to be in close agreement with earlier theoretical prediction and experimental values reported in the literature.

(Some figures in this article are in colour only in the electronic version)

1. Introduction

The rare earth monpnictides and monochalcogenides form a very interesting group of materials. They exhibit a rich variety of anomalous physical properties attracting considerable attention for basic and applied research. Among the rare earth alloys, the isomorphic compounds like $\text{Gd}^{3+}\text{X}_p^{3-}$, where $X_p = \text{N, P, As, Sb, Bi}$, and $\text{Eu}^{2+}\text{X}_c^{2-}$, where $X_c = \text{O, S, Se, Te}$, can be compared since they are isoelectronic in nature. If pure ionic bonding is considered then they are expected to be insulators or semiconductors. The divalent rare earth monochalcogenides are indeed insulators or semiconductors [1, 2] but the trivalent rare earth monpnictides, especially the rare earth nitride GdN, show an intricate conducting character. For instance, the band-structure calculations suggest GdN to be a semiconductor [3–5], a half-metal [6–8] or a semiconductor in the paramagnetic and a semimetal in the ferromagnetic case using quasi-particle self-energy corrections [9]. The above mentioned results used different computational techniques. Hasegawa *et al* [3] were the first to calculate the self-consistent

electronic band structures of GdN for the paramagnetic case using the augmented plane wave (APW) method. Their calculations employed the one-electron potential instead of local spin density (LSD) functional theory. While Lambrecht [4] addressed the problem by estimating the gap corrections beyond the local density approximation (LDA), Ghosh [5] performed self-consistent spin polarized calculations using the full potential linear muffin-tin orbital (FP LMTO) but with rigid shifts in the 5d and 4f states in order to fit the experimental x-ray photoemission spectroscopy (XPS) and x-ray Bremsstrahlung isochromat spectroscopy (BIS) results. The self interaction corrected local spin density (SIC-LSD) calculations by Aerts *et al* [6] and the augmented spherical wave (ASW) within the LDA and generalized gradient approximations (GGA) by Eyert [8] rendered a half-metallic nature to GdN. There has also been an interesting investigation on the electronic structure and magnetic properties of GdN by Duan *et al* [7] based on first principles calculations as a function of unit cell volume. They found that GdN transforms first from half-metallic to semi-metallic and then finally to a semiconductor upon applying stress. These features reveal a strong lattice constant dependence on the electronic structure of GdN. However, experimental results demonstrated bulk GdN to be a low carrier semimetal [10] or GdN thin films to be insulating [11].

The magnetic properties of GdN also form a very interesting study and the mechanism of magnetism is highly intriguing. There had also been a dispute regarding the magnetic properties [10] of GdN, with earlier reports describing it to be an antiferromagnetic [10, 12] material while other studies indicated it to be a ferromagnet [13, 14]. But after such controversial discourse, it has been accepted that stoichiometric GdN is a ferromagnetic [15, 16] material. There have been theoretical attempts in order to explain the magnetism in GdN using the RKKY interaction picture by Kuznietz [17] and a model proposed by Kasuya [18] which is related to the cross processes between the f-d mixing and the f-d exchange interaction. In this paper we do not discuss the mechanism of such anomalous behaviour of magnetic properties in GdN but it forms a part of future investigations. As a whole, it generates a huge motivation to study such an interesting material and understand the physical phenomenon in similar strongly correlated systems.

Here we combine the many-body analysis of the multi-band Kondo lattice model along with the first principles TB-LMTO spin polarized band-structure calculations to investigate the temperature dependent electronic correlation effects in the conduction bands of GdN. We wish to emphasize that upon using band-structure calculations we are not aiming to find the nature of the electronic ground state of GdN but rather take its output as the starting point (input) for our many-body theory and compare the results for the temperature dependence with the experimental ones (redshift phenomenon). Very recently, a similar study has been reported [19] but using a different approach for determining the self-energy [20] and also for the input in the many-body part.

The layout of the paper is as follows. In section 2 we develop the complete multi-band Hamiltonian. A self-energy ansatz, authentic for low carrier densities, is used to solve the model Hamiltonian. In section 3, we present the electronic band structure of the conduction bands of GdN using the tight binding linear muffin-tin orbital (TB LMTO) program within the LSDA and also obtain the inter-band exchange coupling. In the next section 4, the many-body model is combined with first principles $T = 0$ band-structure calculations in order to calculate the temperature dependence of some physical properties like the quasi-particle density of states (Q-DOS), spectral density (SD), quasi-particle band structure (Q-BS) and red-shift phenomenon in ferromagnetic GdN. In the last section 5, we conclude with the proposition of a spin resolved ARIPS experiment to be performed in order to validate our results and thus inspire experimental efforts to be carried out in order to study the intriguing temperature dependent properties of GdN.

2. Theoretical model

The temperature dependent electronic correlation effects in the conduction bands of GdN are due to the exchange interaction between the electron in extended (5d) band states and the localized (4f) electrons which give rise to localized magnetic moments. This situation is covered by the so called ferromagnetic multiband Kondo lattice model (KLM), the Hamiltonian of which reads

$$H = H_{\text{kin}} + H_{\text{int}} \quad (1)$$

where

$$H_{\text{kin}} = \sum_{ij\alpha\beta\sigma} T_{ij}^{\alpha\beta} c_{i\alpha\sigma}^\dagger c_{j\beta\sigma} \quad (2)$$

and

$$H_{\text{int}} = -\frac{J}{2} \sum_{i\alpha\sigma} (z_\sigma S_i^z c_{i\alpha\sigma}^\dagger c_{i\alpha\sigma} + S_i^\sigma c_{i\alpha-\sigma}^\dagger c_{i\alpha\sigma}). \quad (3)$$

The term H_{kin} denotes the kinetic energy of the conduction band electrons, 5d orbitals in the case of GdN, with $c_{i\alpha\sigma}^\dagger$ and $c_{i\alpha\sigma}$ being the fermionic creation and annihilation operators, respectively, at lattice site \mathbf{R}_i . The Latin letters (i, j, \dots) symbolize the crystal lattice indices while the band indices are depicted in Greek letters (α, β, \dots) and the spin is denoted as σ ($=\uparrow, \downarrow$). The multi-band hopping term, $T_{ij}^{\alpha\beta}$, is obtained from an LDA calculation which incorporates in a realistic manner the influences of all those interactions which are not directly accounted for by our model Hamiltonian. It is connected by Fourier transformation to the free Bloch energies $\epsilon^{\alpha\beta}(\mathbf{k})$

$$T_{ij}^{\alpha\beta} = \frac{1}{N} \sum_{\mathbf{k}} \epsilon^{\alpha\beta}(\mathbf{k}) e^{-i\mathbf{k}\cdot(\mathbf{R}_i - \mathbf{R}_j)} \quad (4)$$

H_{int} is an intra-atomic exchange interaction term, being further split into two subterms. The first describes the Ising type interaction between the z -component of the localized and itinerant carrier spins while the other comprises spin exchange processes which are responsible for many of the KLM properties. J is the exchange coupling strength, which we assume to be \mathbf{k} independent, and S_i^σ refers to the localized spin at site \mathbf{R}_i

$$S_i^\sigma = S_i^x + iz_\sigma S_i^y; \quad z_\uparrow = +1, z_\downarrow = -1. \quad (5)$$

The Hamiltonian in equation (1) provokes a nontrivial many-body problem that cannot be solved exactly. The details of the many-body analysis along with a model calculation and limiting cases are explained elsewhere (see [21]). We explain it in brief as follows.

Using the equation of motion method for the double-time retarded Green function [22]

$$G_{lm\sigma}^{\mu\nu}(E) = \langle\langle c_{l\mu\sigma}; c_{m\nu\sigma}^\dagger \rangle\rangle_E \quad (6)$$

where l, m and μ, ν are the lattice and band indices respectively, we obtain higher order Green functions which prevent the direct solution. Approximations must be considered. But, a rather formal solution can be stated as

$$\hat{G}_{\mathbf{k}\sigma}(E) = \hbar \hat{I}[(E + i0^+) \hat{I} - \hat{\epsilon}(\mathbf{k}) - \hat{\Sigma}_{\mathbf{k}\sigma}(E)]^{-1} \quad (7)$$

where we exclude the band indices by representing the terms in a generalized matrix form on symbolizing a hat over it

$$\hat{G}_{lm\sigma}(E) = \frac{1}{N} \sum_{\mathbf{k}} \hat{G}_{\mathbf{k}\sigma}(E) e^{-i\mathbf{k}\cdot(\mathbf{R}_l - \mathbf{R}_m)}. \quad (8)$$

The terms in equation (7) are explained as follows: \hat{I} is an identity matrix and $\hat{\epsilon}(\mathbf{k})$ is a hopping matrix with the diagonal terms of the matrix exemplifying the intra-band hopping and the off-diagonal terms denoting the inter-band hopping. The self-energy, $\hat{\Sigma}_{\mathbf{k}\sigma}(E)$, containing all the influences of the different interactions being of fundamental importance, can be understood using site representation:

$$\langle\langle [H_{\text{int}}, c_{l\mu\sigma}]_-; c_{mv\sigma}^\dagger \rangle\rangle = \sum_{p\gamma} \Sigma_{lp\sigma}^{\mu\gamma}(E) G_{pm\sigma}^{\gamma\nu}(E). \quad (9)$$

Now, we are left with the problem of finding a multi-band self-energy ansatz in order to compute the Green function matrix and thereby calculate the physical quantities of interest like the quasi-particle spectral density (SD)

$$A_{\mathbf{k}\sigma}(E) = -\frac{1}{\pi} \text{Im Tr}(\hat{G}_{\mathbf{k}\sigma}(E)) \quad (10)$$

and the quasi-particle density of states (Q-DOS)

$$\rho_\sigma(E) = \frac{1}{N\hbar} \sum_{\mathbf{k}} A_{\mathbf{k}\sigma}(E). \quad (11)$$

According to our many-body theoretical analysis [21], we utilize the multi-band interpolating self-energy ansatz (ISA), which is accurately defined in the low carrier density regime, for all coupling strengths and satisfying various limiting cases of the model like the one of a ferromagnetically saturated semiconductor as discussed in the appendix of reference [21]. The ansatz is given as

$$\hat{\Sigma}_\sigma(E) = -\frac{J}{2} M_\sigma \hat{I} + \frac{J^2}{4} a_\sigma \hat{G}_\sigma \left(E - \frac{J}{2} M_\sigma \right) \left[\hat{I} - \frac{J}{2} \hat{G}_\sigma \left(E - \frac{J}{2} M_\sigma \right) \right]^{-1} \quad (12)$$

where

$$M_\sigma = z_\sigma \langle S^z \rangle; \quad a_\sigma = S(S+1) - M_\sigma(M_\sigma + 1). \quad (13)$$

and the bare Green function matrix is defined as

$$\hat{G}_\sigma(E) = \frac{1}{N} \sum_{\mathbf{k}} \frac{1}{(E + i0^+) \hat{I} - \hat{\epsilon}(\mathbf{k})}. \quad (14)$$

As seen in equation (12), we are interested only in the local self-energy

$$\hat{\Sigma}_\sigma(E) = \frac{1}{N} \sum_{\mathbf{k}} \hat{\Sigma}_{\mathbf{k}\sigma}(E). \quad (15)$$

The wavevector dependence of the self-energy is mainly due to the magnon energies $\hbar\omega(\mathbf{k})$ appearing at finite temperature. But, we neglect a direct Heisenberg exchange between the localized spins since we are only interested in the influence of inter-band exchange on the conduction band states in order to study the electronic correlations and not aimed at calculating the magnetic properties via self-consistent calculation of localized magnetizations. This can be interpreted as the $\hbar\omega(\mathbf{k}) \rightarrow 0$ limit. The localized magnetization $\langle S^z \rangle$ shall be considered as an external parameter responsible for the induced temperature dependence of the band states.

3. Band-structure calculation

In order to have the single-particle excitation energies, i.e. the hopping matrices, which act as an input in the many-body part, and also to find the exchange coupling strength, we perform the TB-LMTO [23, 24] band-structure calculations within LDA. GdN crystallizes in a rock-salt

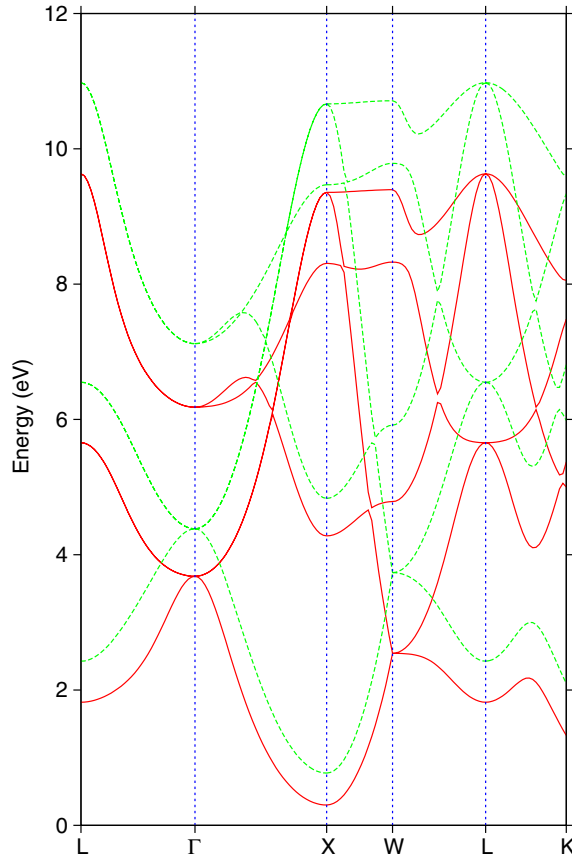


Figure 1. LDA band structure of 5d conduction bands of GdN. Full (red) lines are spin \uparrow and dotted (green) ones are spin \downarrow .

structure with an experimental lattice constant of 4.99 Å and symmetry group $Fm\bar{3}m$. Each Gd^{3+} ion has 12 nearest and six next nearest Gd neighbours.

Figure 1 indicates the calculated spin-dependent 5d conduction bands of GdN. Our evaluation is restricted only to 5d bands while considering GdN to be a semiconductor in accordance with [3–5]. But, even after making such simplifications in our calculation, there are typical difficulties due to the LDA which arise in the treatment of the strongly localized character of the 4f levels. In order to circumvent this problem we considered the 4f electrons as core electrons, since our main interest is focused on the response of the conduction bands on the magnetic state of the localized moments. For our purpose, the 4f levels appear only as localized spins. Moreover, since we are mainly concerned with overall temperature dependent correlation effects, the extreme details of the band structure are surely not so important.

In figure 2 the LDA density of states is displayed. A distinct exchange splitting is visible which can be used to fix the interband exchange coupling constant J in equation (3). Assuming that the LDA treatment of the ferromagnetism is quite compatible with the Stoner (mean field) picture, the $T = 0$ splitting amounts to $\Delta E = JS$. On taking the centre of gravity of both the bands and along with the above assumption we obtain

$$\Delta E = 1.237 \text{ eV} \Rightarrow J = 0.35 \text{ eV}. \quad (16)$$

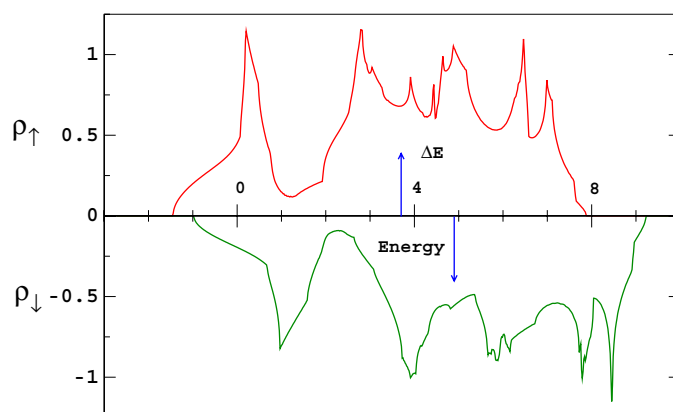


Figure 2. Spin-dependent density of states of 5d bands of GdN. Using the centre of gravity of the bands, the exchange splitting amounts to $\Delta E = 1.237$ eV.

In the band-structure calculations, one cannot switch off the inter-band exchange interaction (equation (3)) in the LDA code, but one can speculate from the exact $T = 0$ result for the empty conduction band [25] that such an interaction leads only to a rigid shift in the \uparrow spectrum while the \downarrow spectrum is remarkably deformed by correlation effects due to spin exchange processes between the delocalized and localized states. So we take from the LDA calculation, which holds by definition for $T = 0$, the \uparrow part as the single-particle input in equation (2). Therewith, it is guaranteed that all other interactions which do not explicitly come into our Hamiltonian are implicitly taken into account by the LDA single-particle Hamiltonian. On the other hand, a double counting of any decisive interaction is avoided since in the \uparrow -spectrum the inter-band exchange (equation (3)) only shifts the energy zero. Since the methodology used in [19] remains the same, it is worthwhile to mention that the authors have used paramagnetic band structure as an input in their many-body part, though it is not guaranteed that the paramagnetic input is free of correlation effects.

In order to get a first impression of the correlation effects we have evaluated our theory for $T = 0$ K and the results are presented in figure 3. The \uparrow spectrum is unaffected by the actual value of J and coincides with the respective LDA curve, after a compensation of the unimportant rigid shift ($\frac{JS}{2}$). The slight deviations seen in the upper part of figure 3 are exclusively due to numerical procedures. This shows that our theoretical approach for implementing LDA input into the many-body model fulfils the exact limit ($T = 0$, $\sigma = \uparrow$) and also circumvents the earlier mentioned double-counting problem. The lower half, \downarrow spectrum, of figure 3 demonstrates that correlation effects do appear even at $T = 0$ K. Apart from a band narrowing, they provoke strong deformations and shifts with respect to the LDA result.

4. Model evaluation

In this section, we present the numerical results emphasizing the temperature dependent electronic correlation effects in the conduction bands of GdN by combining the first principles TB LMTO band-structure calculations within the LSDA along with the many-body theoretical model.

The correlation effects are examined as the consequence of a test electron created (or annihilated) in an empty (or filled) band. In our case, we create an electron in an empty conduction band with a consideration of GdN as a ferromagnetic semiconductor. Such effects

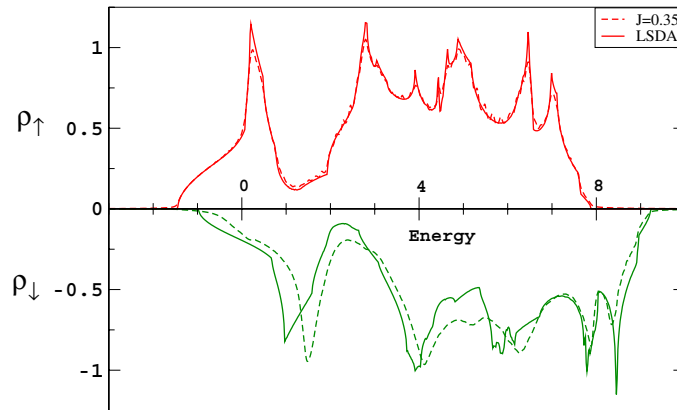


Figure 3. The same as in figure 2 with additional $T = 0$ results of our combined many-body and first principles theory for exchange coupling $J = 0.35$ eV, shown in broken lines.

are studied by calculating the single-electron Green function (equation (7)). But, apart from the electronic sub-system, we also have the magnetic sub-system. The exchange coupling between the itinerant electron and localized spins adds to the correlation effects as they produce spin-flip transitions and Ising-like interactions in addition to the kinetic energy.

The numerical calculations remain the same as performed in [21]. For the sake of brevity, one can understand it as follows. The single-particle output obtained from the band-structure calculations is in the form of a Hamiltonian and overlap matrix, posing a generalized eigenvalue problem to be solved. In order to employ such matrices as an input for the many-body calculations, one has to perform a decomposition so as to reduce the generalized problem to an eigenvalue problem. Using such an approach, one can factorize the Hamiltonian matrices and then obtain new Hamiltonian matrices using overlap matrices which can be used directly as hopping integrals, $\hat{\epsilon}(\mathbf{k})$. This factorization and direct use of Hamiltonian matrices circumvent the problem of the somewhat ambiguous decomposition of the conduction band [26–28] into single non-degenerate subbands which is also used in [19]. Finally, we use the multi-band self-energy ansatz (equation (12)) to compute the Green function (equation (7)) and therewith calculate the spectral densities (equation (10)) and densities of states (equation (11)).

The quasi-particle density of states (Q-DOS) are calculated for $J = 0.35$ eV and plotted in figure 4 for various values of 4f magnetizations, i.e. different temperatures. As observed (from the inset of figure 4), the lower edge of spin- \uparrow Q-DOS performs a shift to lower energies upon cooling from $T = T_c$ down to $T = 0$ K, which explains the redshift effect of the optical absorption edge for an electronic transition. We find a redshift of 0.34 eV. One should note that a simple mean field treatment with $J = 0.35$ eV and $S = 3.5$ would result in a redshift of 0.6125 eV. Obviously, the correlation effects drastically reduce this value. A similar redshift phenomenon was discussed by Lambrecht [4], with a calculated value of 0.30 eV, and was also reported experimentally, having a value of 0.40 eV, by Leuenberger [16]. They observed this effect as a shift of the L_2 edge in a relative comparison between absorption spectra measured on a 2000 Å GdN film at $T > T_c$ and $T < T_c$ in an x-ray magnetic circular dichroism (XMCD) experiment. The L_2 absorption spectrum is sensitive to the polarization of t_{2g} states. In [19], the redshift of 0.483 eV was obtained using J for the lowest band of the bulk GdN and was found to be overestimated.

Figure 5 represents the quasi-particle band structure for some high symmetry directions in the first Brillouin zone. The degree of blackening measures the magnitude of the spectral

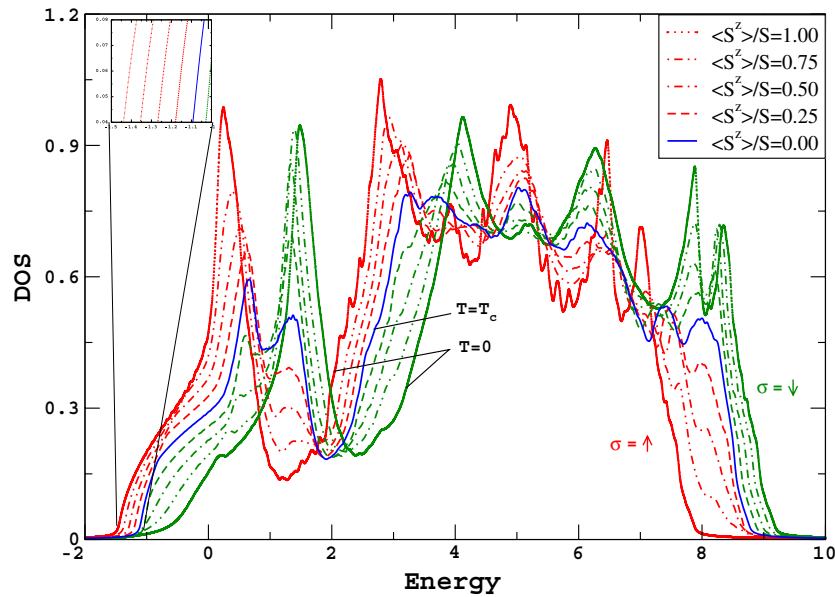


Figure 4. Quasi-particle density of states (Q-DOS) of the 5d conduction bands of GdN and as a function of energy for various temperatures (different 4f magnetizations). The outermost curves belong to $T = 0$ K ($\frac{\langle S^z \rangle}{S} = 1$). On increasing the temperature they approach each other. The inset shows on an enlarged scale the temperature shift of the lower edge for the case of \uparrow .

function. As observed in the \downarrow spectrum even at $T = 0$ K ($\frac{\langle S^z \rangle}{S} = 1$), parts of the dispersions are washed out, showing lifetime effects due to correlation in terms of magnon emission and re-absorption with simultaneous spin-flips which can be understood as follows.

At $T = 0$ K and empty bands, the addition of a \uparrow electron produces a stable quasi-particle since the \uparrow electron has no chance to flip its spin with the ferromagnetically saturated spin ($\uparrow\uparrow$) sub-system. The imaginary part of the self-energy vanishes, indicating infinite lifetimes. The situation is different for the addition of an \downarrow electron as the \downarrow electron can exchange its spin with the ferromagnetically saturated spin sub-system and have finite lifetime. It can emit a magnon and become a \uparrow electron provided there exist \uparrow electron states which can be occupied after the spin-flip process. These are the scattering states which occupy the same energy regions as the \uparrow spectrum. The other possibility for the \downarrow electron to exchange its spin could be by repeated emission and absorption of magnons, thus forming a quasi-particle called the magnetic polaron. For strong coupling, the above mentioned elementary processes can even lead to correlation caused splitting of the dispersion. This is clearly visible in certain parts of figure 5.

For finite temperatures, the spin sub-system is no longer perfectly aligned. There are magnons in the system that can be absorbed by the itinerant charge carriers provoking quasi-particle damping in the \uparrow spectrum too. The spectral weight gets redistributed due to the spin flip term in the exchange interaction with deformations in the density of states. The overall exchange splitting reduces with increasing temperature, until in the limit $T \rightarrow T_c$ ($\langle S^z \rangle \rightarrow 0$) the vanishing 4f magnetization removes the induced spin asymmetry.

In order to have a closer look at the correlations, the spin and \mathbf{k} -dependent spectral densities are plotted at some high symmetry points (W, K, X) in the first Brillouin zone and for different temperatures. While the Q-DOS refer to an angle averaged photoemission experiment, the \mathbf{k} -dependent spectral densities refer to the angle resolved part.

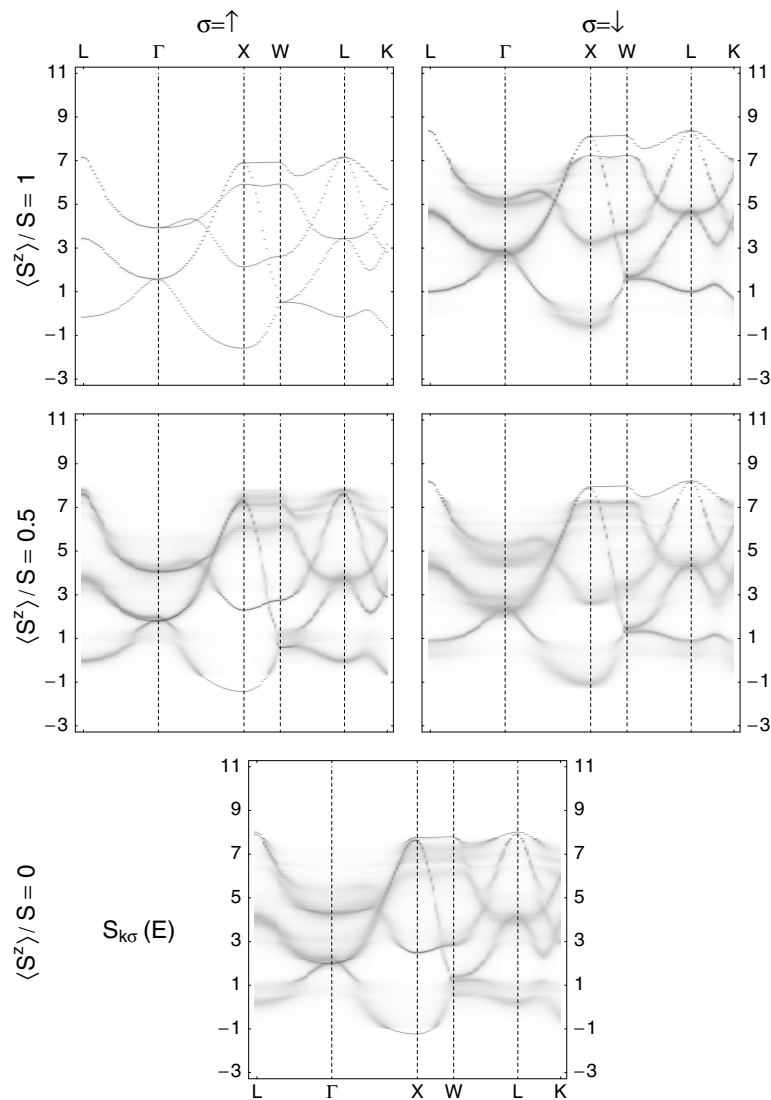


Figure 5. Spin-dependent quasi-particle band structure of 5d conduction bands of GdN for different values of magnetization $\frac{\langle S^z \rangle}{S}$.

As seen in figure 6, well defined quasi-particle peaks appear with an additional spin split below T_c . In accordance with the quasi-particle band structure, it is observed in figure 6 that four sharp peaks appear at $T = 0$ K for the \uparrow spectrum, and though already strongly damped (at lower energies) the same peak sequence comes out in the \downarrow spectrum. The exchange splitting collapses for $T \rightarrow T_c$ and the quasi-particle damping increases with increasing temperature. For $T = T_c$ (full lines), the spectrum is washed out at higher energies, exhibiting strong correlation effects.

Similar explanations hold for the other high symmetry points (figures 7 and 8). There is a strong damping as seen along the entire energy spectrum. Moreover, some of the peaks (lower energy peaks in figure 7) are so strongly damped that they may not be visible in the inverse

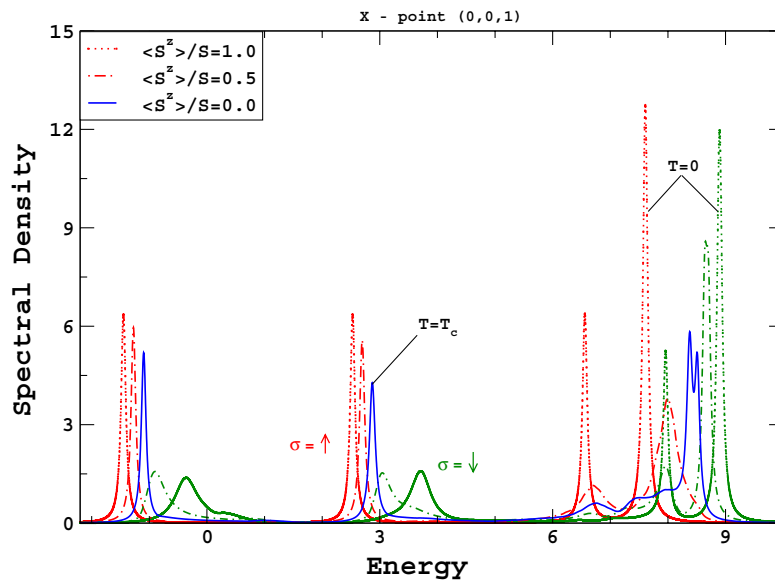


Figure 6. Spectral density at the X point. The case of $\frac{\langle S^z \rangle}{S} = 1.0$ is shown by dotted lines, while $\frac{\langle S^z \rangle}{S} = 0.50$ is denoted as broken lines and the full lines represent $\frac{\langle S^z \rangle}{S} = 0.0$.

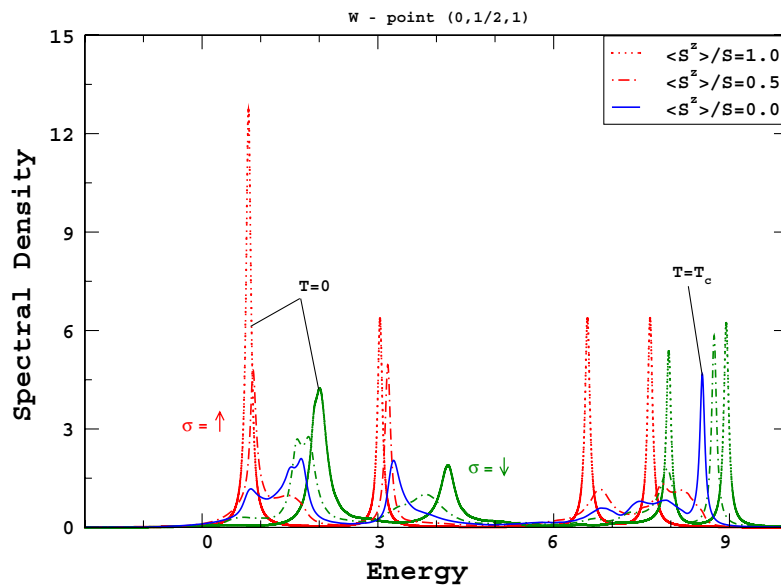


Figure 7. The same as in figure 6 but for the W point.

photoemission experiment. Altogether, the 5d spectral densities exhibit drastic temperature dependences, which concerns the positions and the widths of quasi-particle peaks.

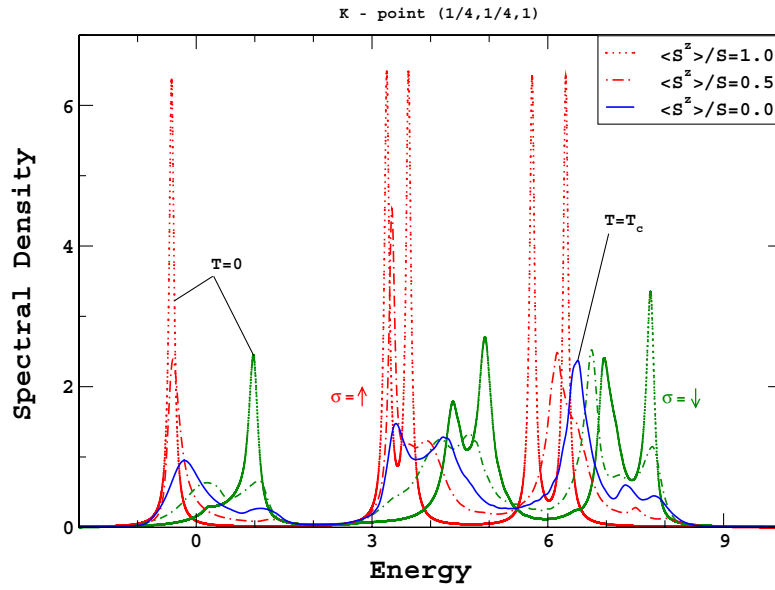


Figure 8. The same as in figure 6 but for the K point.

5. Summary and conclusion

We investigated the temperature dependent electronic correlation effects on the 5d conduction bands of GdN. In this respect, we started with a multi-band Kondo lattice Hamiltonian which describes an exchange interaction between the localized moments and itinerant conduction electrons. Using the equation of motion approach in terms of the Green function, we tried to evaluate the multi-band KLM Hamiltonian. In order to find the solution, i.e. the Green function, there was a need to find a self-energy ansatz which incorporated all the interactions of the system. We used an interpolating self-energy ansatz (ISA) [25] for the multi-band [21] case which was found to be reliable for low carrier densities and all coupling strengths and which fulfilled important limiting cases of the model.

We further performed band-structure calculations using the TB LMTO program in order to obtain hopping matrices, which served as an input in the many-body analysis. Though there has been a wide discrepancy regarding the nature of the electronic ground state of GdN, we considered it to be a semiconductor and thereby concentrated only on the empty 5d bands and the correlation effects due to their interaction with 4f localized moments. From the band-structure calculations, we also obtained the inter-band exchange coupling strength as a consequence of exchange based splitting of the 5d conduction bands.

The first principles band-structure calculations were combined with the many-body theory in order to calculate the Green function and therewith some of the physical properties of interest in GdN like quasi-particle spectral densities (Q-SD) and densities of states (Q-DOS) are estimated for different values of magnetization and exchange coupling strength. A redshift of 0.34 eV for exchange coupling $J = 0.35$ eV was calculated and found to be in close agreement with other theoretical prediction and experimental values reported in the literature. Strong temperature dependent correlation effects were observed over the whole energy spectrum. Our results can be compared with spin dependent ARIPS of the conduction bands of GdN and thus we would like to instigate experimental efforts in order to study this interesting compound.

Acknowledgments

We would like to thank Professor P A Dowben (UNL, USA), Professor W R L Lambrecht (CWRU, USA) and PD Dr V Eyert (Universität Augsburg, Germany) for helpful discussions and comments on the electronic band structure of GdN.

References

- [1] Wachter P 1979 *Handbook on the Physics and Chemistry of Rare Earth* vol 2, ed K A Gschneider Jr. and L Eyring (Amsterdam: North-Holland) chapter 19
- [2] Mauger A and Godart C 1986 *Phys. Rep.* **141** 51–176 (Review Section of Physics Letters)
- [3] Hasegawa A and Yanase A 1976 *J. Phys. Soc. Japan* **42** 493
- [4] Lambrecht W R L 2000 *Phys. Rev. B* **62** 13538
- [5] Ghosh D B, De M and De S K 2005 *Phys. Rev. B* **72** 45140
- [6] Aerts C M, Strange P, Horne M, Temmerman W M, Szotek Z and Svane A 2004 *Phys. Rev. B* **69** 45115
- [7] Duan C-g, Sabiryanov R F, Liu J, Mei W N, Dowben P A and Hardy J R 2005 *Phys. Rev. Lett.* **94** 237201
- [8] Eyert V 2006 private communication
- [9] Petukhov A G, Lambrecht W R L and Segall B 1996 *Phys. Rev. B* **53** 4324
- [10] Wachter P and Kaldis E 1980 *Solid State Commun.* **34** 241
- [11] Xiao J Q and Chien C L 1996 *Phys. Rev. Lett.* **76** 1727
- [12] Cutler R A and Lawson A W 1975 *J. Appl. Phys.* **46** 2739
- [13] Boyd E L and Gambino R J 1964 *Phys. Rev. Lett.* **12** 20
- [14] Gambino R J, McGuire T R, Alperin H A and Pickart S J 1970 *J. Appl. Phys.* **41** 933
- [15] Li D X, Haga Y, Shida H, Suzuki T, Kwon Y S and Kido G 1997 *J. Phys.: Condens. Matter* **9** 10777
- [16] See Figure 4.14 in Leuenberger F 2004 *PhD Thesis* Georg-August-Universität zu Göttingen (<http://webdoc.sub.gwdg.de/diss/2004/leuenberger/leuenberger.pdf>)
- [17] Kuznietz M 1971 *J. Appl. Phys.* **42** 1470
- [18] Kasuya T and Li D X 1997 *J. Magn. Magn. Mater.* **167** L1
- [19] Bhattacharjee S and Jaya S M 2006 *Eur. J. Phys. B* **49** 305
- [20] Nolting W, Jaya S M and Rex S 1996 *Phys. Rev. B* **54** 14455
- [21] Sharma A and Nolting W 2006 *Phys. Status Solidi b* **243** 641
- [22] Zubarev D N 1960 *Usp. Fiz. Nauk* **71** 71
Zubarev D N 1960 *Sov. Phys.—Usp.* **3** 320 (Engl. Transl.)
- [23] Andersen O K 1975 *Phys. Rev. B* **12** 3060
- [24] Andersen O K and Jepsen O 1984 *Phys. Rev. Lett.* **53** 2571
- [25] Nolting W, Reddy G G, Ramakanth A and Meyer D 2001 *Phys. Rev. Lett.* **64** 155109
- [26] Nolting W, Borgiel W and Borstel G 1988 *Phys. Rev. B* **37** 7663
- [27] Rex S, Eyert V and Nolting W 1999 *J. Magn. Magn. Mater.* **192** 529
- [28] Santos C, Eyert V and Nolting W 2004 *Phys. Rev. B* **69** 214412